Cooperative Research and Development Agreement Final Report

CRADA Number	2707
CRADA Title	Advanced Stability Analysis for Magnetized Target Fusion
National Laboratory Principal Investigator	Princeton Plasma Physics Laboratory Chang Liu cliu@pppl.gov
Contractor	Princeton University Dylan Brennan dylanb@princeton.edu
Company	General Fusion Corp., DUNS 117111477
Company Principal Investigator	Matt Miles matt.miles@generalfusion.com Aaron Froese aaron.froese@generalfusion.com
Award	INFUSE 2020 Round 1
Period of Performance	2021 August 23 – 2022 November 23
Final Report Submission Date	2024 February

Joint Work Statement Funding table showing DOE funding commitment:

Budget and Reporting Code:	AT1050000
Headquarters Program Manager:	Daniel Clark
Headquarters Organization:	SC-24 Fusion Energy Sciences
Contractor Work Proposal Manager:	Chang Liu
Contractor Name:	Princeton Plasma Physics Laboratory
Funding Summary (BA):	FY 2020: $160,000
Cost Sharing Requirements:	FY 2020: $75,000 in-kind contributions

Abstract:
The Princeton Plasma Physics Laboratory (PPPL) is partnering with General Fusion on an INFUSE 2020 award titled "Advanced Stability Analysis for Magnetized Target Fusion". The work will be performed under a Cooperative Research and Development Agreement (CRADA). This Field Work Proposal addresses the PPPL work scope for the funding being provided by the Fusion Energy Sciences program.

The concept of using compression for the heating of closed-flux magnetized plasmas dates back decades. Compression is attractive for heating because of the high power that can be delivered and because compression can be achieved through a liquid metal blanket, as in the General Fusion Magnetized Target Fusion (MTF) approach. Many novel fusion concepts are in the MTF/Magneto-Inertial Fusion regime and propose to use compact toroid plasma targets. This project will deliver an enhanced modeling toolset for understanding the MHD stability of these magnetized targets during compression.

Executive Summary of CRADA Work:

The Cooperative Research and Development Agreement (CRADA) between Princeton Plasma Physics Laboratory (PPPL) and General Fusion Inc. (GF) focused on applying advanced computational stability analyses to plasma equilibria that are expected in the Fusion Demonstration Plant (FDP) device being designed by General Fusion. The FDP is a Magnetized Target Fusion concept that compresses a toroidal plasma to fusion conditions inside of a liquid lithium blanket. The pressure-driven interchange modes were investigated using M3D-C1 code developed at PPPL, including the linear growth and nonlinear saturation. In particular, building on encouraging initial analyses, the effect of plasma rotation on the stability was studied using the Resistive DCON and NIMROD. The results have helped to inform General Fusion on how to maintain stable plasma equilibria during the operation of MTF devices.

Summary of Research Results:

1. BACKGROUND

General Fusion is pursuing a Magnetized Target Fusion (MTF) approach for developing a practical, commercially viable path to fusion energy that involves compressing an initial magnetically confined plasma inside a cavity formed in liquid metal.

Compressing a plasma using a liquid metal flux conserver (FC) to increase its temperature and density addresses many of the problems facing proposed fusion energy sources, such as tritium breeding, component degradation by neutron irradiation, and high cost [Laberge 2008]. With reasonably good plasma confinement, the heating is quasi-adiabatic and fusion-relevant conditions can be attained. An important requirement for successful MTF is that the plasma remains MHD stable during the compression, since instabilities usually lower the plasma temperature resulting in decreased energy production. However, there are a number of compression effects that may cause the plasma to become unstable. These include the changing current profile due to evolution of the FC geometry and the increase of plasma beta. To properly design and successfully operate the FDP it is necessary to understand the plasma stability for the entire compression.

Understanding the stability of magnetized plasma has been a significant challenge of physics for many decades and is still a subject of intense research at national laboratories. During the Project, General Fusion and PPPL applied existing stability theory to plasma compression scenarios to gain insight into the stability of compressed plasmas and improve the design of a successful MTF device. General Fusion and PPPL produced a set of software tools to analyze the stability of plasmas undergoing compression to fusion conditions.

Encouraging early results were first presented at the 2018 APS-DPP meeting [Froese 2018], based on analyses using the DCON code [Glasser 2016a]. Operational pathways were found where ideal MHD modes are stable through to high compression. For multiple compression geometries, sequences of equilibria were generated using the CORSICA [Crotinger 1997] code under the assumptions of ideal and adiabatic compression; both the safety factor profile, $q(\psi, t)$,

and entropy profile, $S(\psi, t)$, were assumed to be unchanging. Each equilibrium was then tested with DCON to determine its ideal MHD stability. The initial plasma pressure and current density profiles were varied to determine the robustness of the stability boundaries. Geometry was found to affect the stability only to the extent that the starting q profile was modified. Many cases with $q_0 > 1$ were found to be n=1 stable, but still susceptible to intermediate modes at high compression. Under certain conditions involving geometry and profile structure, configurations were found to be ideal stable throughout the compression, offering an ideal MHD stable path to high compression.

Results from the first application of Resistive DCON (RDCON) [Glasser 2016b] to General Fusion's compression geometries were also presented [Froese 2018]. Many of the regions in parameter space which were ideal MHD stable actually exhibited resistive instability before maximum compression was reached. However, some narrow pathways remained that permitted a stable plasma to be fully compressed. Plasma rotation has a generally stabilizing effect, so it was expected that adding rotation to the analysis would widen those pathways. However, this was found to be a weak effect.

This Project uses NIMROD [Sovinec 2004] to evaluate error field penetration, including the effects of plasma rotation, and M3D-C1 [Jardin 2004] to evaluate soft-beta limits. Chang Liu is one of the major developers of M3D-C1. Dylan Brennan is an expert on NIMROD, resistive MHD physics and familiar with compact toroid experiments. They are uniquely skilled to make the changes necessary to apply M3D-C1 and NIMROD to plasma compression. They provided valuable technical and physics support for applying NIMROD, M3D-C1 and RDCON to MTF experiments.

2. STATEMENT OF OBJECTIVES

The overarching goal of this Project is to explore MTF plasma compression trajectories and identify those that maintain the plasma in a stable state. The effects of greatest interest are:

1. ideal MHD stability
2. resistive tearing and interchange stability
3. the response of the plasma to pressure-driven instabilities
4. stabilization by toroidal rotation
5. applied and error field penetration

As each analysis is performed, viable operating space is identified, and we can refine the engineering requirements for bringing the plasma to fusion conditions.

General Fusion Tasks

- Develop scripts for batch-running CORSICA, RDCON, and RMATCH codes to imitate the physical processes occurring in General Fusion experiments.
- Provide access to and support for the General Fusion high-performance computing resources.
- Provide 3D MHD simulation results from VAC as initial conditions for the stability maps. The VAC results will also be used to compare plasma evolution to the locked-q-profile evolution.

PPPL Tasks

- Run M3D-C1 code to evaluate soft beta limits in an MTF compression experiment.

- Analyze equilibrium plasma states from CORSICA and MHD simulations with VAC for ideal and resistive instability using RDCON and NIMROD. Compare the effects of toroidal rotation between RDCON and NIMROD.

Deliverables

- Set of software tools to analyze the stability of plasmas undergoing compression to fusion conditions.
- A final report summarizing the results of the work performed.

3. TECHNICAL DISCUSSION OF WORK PERFORMED

A. Effect of plasma rotation on stability - written by Aaron Froese

The Project's plasma stability research is intended to support analysis of past experimental results at General Fusion and inform future designs. A series of compression geometries for a simplified FDP design is shown in Fig. 1. A magnetized plasma with closed flux surfaces is confined by image currents induced in the surrounding liquid metal. As the liquid metal collapses the cavity in which the plasma is confined, the inductance decreases, the magnetic field increases, and the plasma is compressed to smaller size by $E \times B$ drift [Liu 2008, Wang 2018]. Plasma mass and entropy are conserved (to a degree determined by transport losses) and so the density and temperature increase. In the adiabatic limit of perfect confinement, the scaling for a spherical collapse is $n \propto R^{-3}$ and $T \propto R^{-2}$, where R is the radius of the cavity. The collapse shown in Fig. 1 is desirable because it is relatively self-similar, but the shape of the plasma cross-section can change significantly in realizable compression schemes.

Proper evaluation of plasma stability in this system requires a time-evolving 3D MHD simulation. General Fusion performs such studies using VAC [Tóth 1996] and NIMROD. However, these codes are computationally intensive. A faster method is required to optimize design parameters like the FC geometry and initial plasma profiles. Therefore, we use an approach based on stability analysis of Grad-Shafranov equilibrium states. The assumption that the equilibrium state is relevant is supported by the fact that the Alfvén time in the experiment is always much shorter than the compression time. Thus, the experiment is in quasi-equilibrium throughout the compression. To model a compression in this way we use CORSICA to generate equilibria for a series of compression ratios $C \propto R_0/R$, where R_0 is the initial major radius of the experiment. Based on an initial plasma equilibrium in uncompressed geometry, subsequent equilibria in compressed geometries are generated by assuming adiabatic compression, so the confined entropy and safety factor profiles are conserved. This is considered a good upper bound on the thermal confinement during a fast compression.

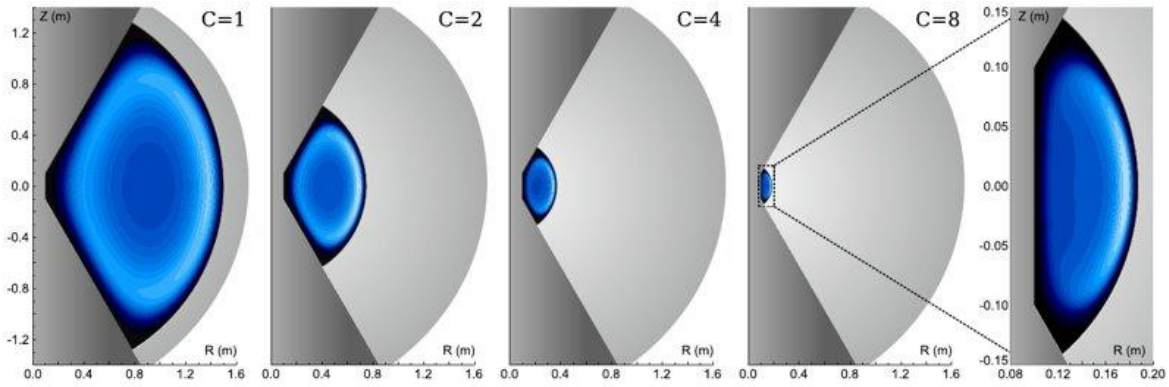

FIG. 1. CORSICA equilibria showing compression of plasma by converging liquid metal flow. Contours indicate normalized parallel current density, $J_{||}/B$. The liquid metal is light gray and solid metal is dark gray.

We begin with an array of initial plasma states by varying the imposed shaft current. The shaft current creates a toroidal field according to $B_\varphi = \mu_0 I_{sh}/2\pi R$. So-called "stability maps" are overlaid contour plots that are created by orienting the initial shaft current along the vertical axis and the compression ratio along the horizontal axis. Fig. 2 is a stability map showing contours for ideal and resistive MHD stability, plasma temperature, and points on the safety factor profile: q_0, q_{min}, and q_{95}. For each initial shaft current indicated on the vertical axis, each point along a horizontal line rightward of this axis is compressed by a factor of R_0/R as indicated on the horizontal axis, with the equilibrium including fields and profiles based on the adiabatic assumption. Thus, the toroidal field along the horizontal direction is greater than that specified on the left axis, though the label of the initial shaft current is informative. Horizontal paths through these maps represent adiabatic compression trajectories. Realistic compressions that include losses will naturally traverse parameter space in a more complex way, but these maps give us a good idea of which design parameters are important.

Each point in the map is an equilibrium that we evaluate with RDCON to get its linear resistive MHD stability. RDCON analyzes an axisymmetric toroidal plasma based on the method of matched asymptotic expansions. The plasma is partitioned into a set of ideal MHD outer regions, connected through resistive MHD inner regions around rational q surfaces. The outer regions satisfy the ideal MHD equations by minimizing the potential energy while the inner regions satisfy the resistive MHD equations to determine the eigenvalue. All regions are solved numerically by singular Galerkin methods, which are fast and robust, which is desirable when applying them to the strongly shaped plasma equilibria that exist in General Fusion devices.

Resistive mode eigenvalues are represented by the multiple complex roots of the RDCON dispersion relation. The list of physical solutions is sorted to return the one with the largest real part of the root, i.e., the fastest growth rate that is slower than ideal timescales, or least stable mode. This is the resistive growth rate that is plotted on the stability map in the colored contours of Fig. 2. For the unstable cases, the frequency of the mode tends to be near zero, while for the near marginal and stable solutions the frequency can be significant. This point is consistent with theoretical literature on resistive MHD instabilities, building confidence in these results.

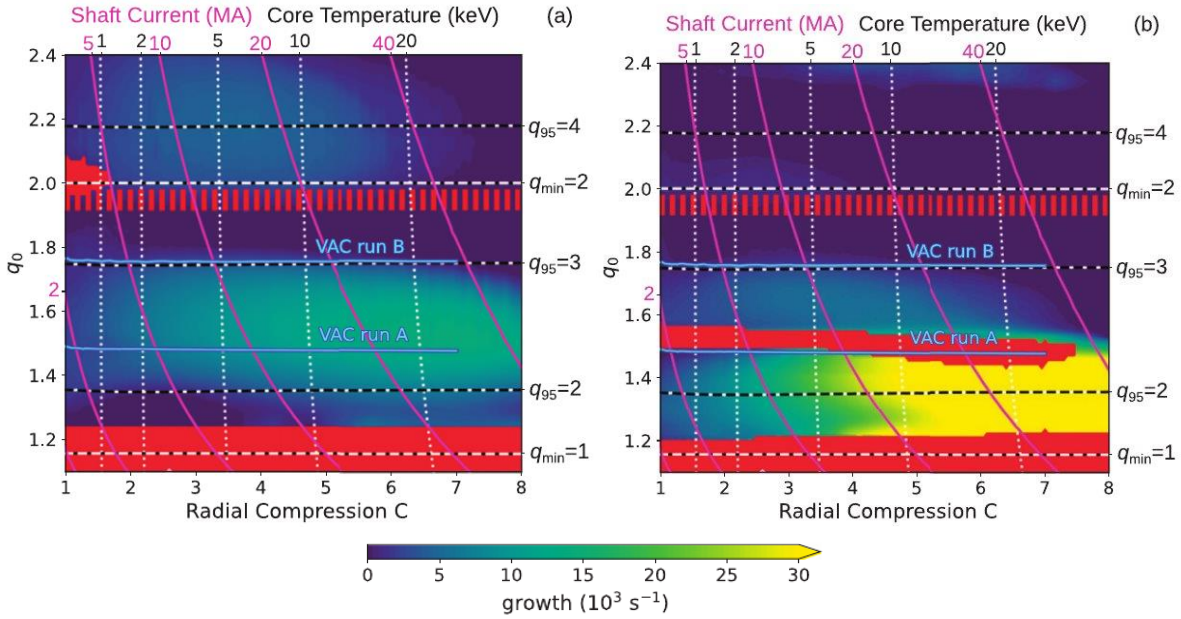

FIG. 2. Stability results from RDCON showing (a) n=1 and (b) n=2 modes in an MTF prototype-sized device. Regions of ideal instability are shoin red, resistive instability in green/yellow, and stability in dark blue. Dotted white contours indicate plasma core temperature in keV. Safety factor values are shown as dashed white (q_0), solid black (q_{min}), and solid gray (q_{95}) contours. Trajectory from two VAC MHD simulations are shown as blue lines.

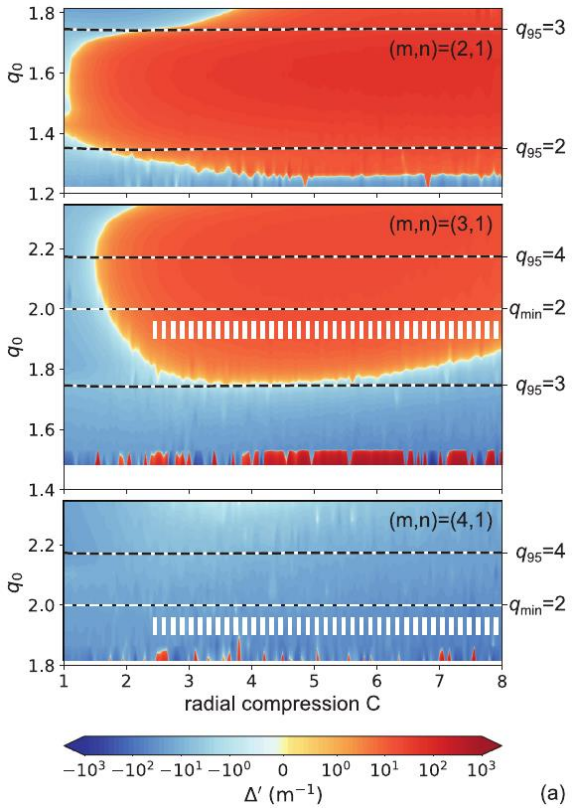

FIG. 3. The resistive stability index Δ' of the 2/1 and 3/1 mode components for the cases analyzed by RDCON in Fig. 2. Cases above and below the colored zone have no q = 2 or q = 3 surface, respectively.

Fig. 3 shows the stability index Δ′ for the *m*/*n* = 2/1 and 3/1 mode components leading to the growth rates shown in Fig. 2. The growth rate in Fig. 2 is calculated from the matrix determinant solution including the coupling between all toroidal mode components of *n* = 1 and including toroidal effects in the layer solution. The resonant lowest *m* modes clearly indicate the dominant outcome behind the physics in the result. Both the coupling between components of different *m* and the toroidal layer effects can significantly change the stability from what would be expected from the local Δ′ alone. In the cases under study, these effects are summarily a stabilizing influence. This is indicated by regions where the 2/1 or 3/1 Δ′ is significantly positive, though the mode remains stable. Much remains to be investigated in these complex results.

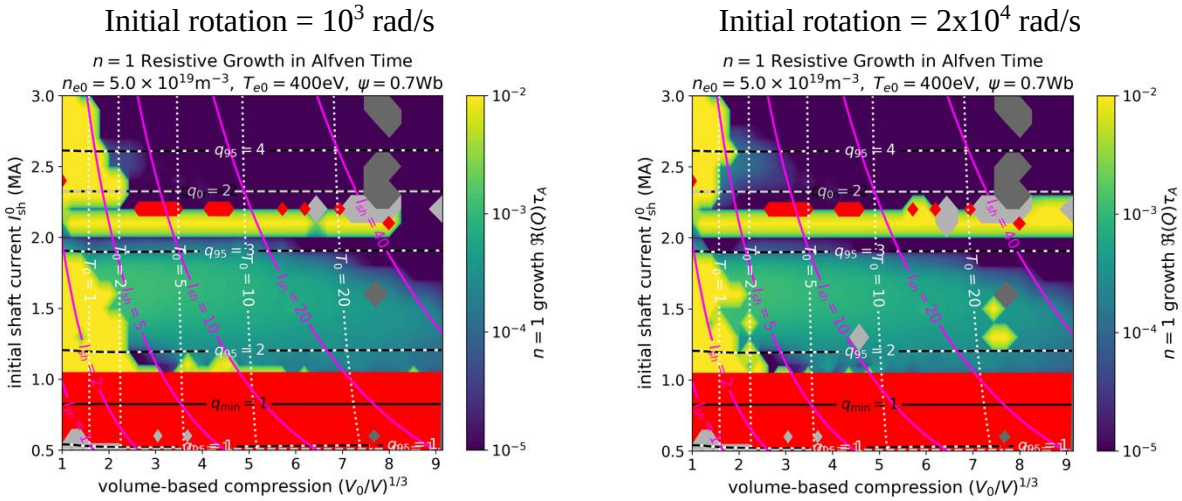

FIG. 4. Stability maps showing negligible effect of rotation on most compression trajectories.

Toroidal rotation increases substantially as compression progresses due to angular momentum conservation alone. This has the effect of increasing the differential in rotation between resonant surfaces of the resistive and ideal MHD instabilities, which is often stabilizing but can destabilize the plasma [Weller 1998]. Though dissipative effects will reduce the attained rotation, an estimation of the increase may be made by assuming rotation speed scales inversely to major radius during compression.

Rotation has a critical effect on the stability of resistive MHD modes [Chu 1999, Hao 2014, Li 2017]. Though the stability to resistive wall modes is relatively assured by the short timescale compression (relative to the wall time) with a thick conducting shell, the differential rotation between surfaces is expected to have a substantially stabilizing effect. In particular, the coupling between individual poloidal components (*m* = 1, 2, . . .) of the mode is expected to be substantially weakened by the differential rotation between surfaces, though the shear in the flow at each rational surface can also have a destabilizing influence [Chen 1990, Chandra 2005]. In Fig. 2, the upper unstable zone in the map is the result of coupling between the 3/1 and 2/1 surfaces. In this Project, rotation rates consistent with that measured in the PI3 experiment (up to 10^4 rad/s) were found to be stabilizing, but typically had a very small effect, as seen in Fig. 4.

B. Analysis of Pressure-driven MHD modes in MTF - written by Chang Liu

In previous work of linear MHD stability analysis using RDCON, a stability map of n=1 mode was generated and stable corridors for different compression ratios were identified. These findings laid the groundwork for subsequent nonlinear MHD simulations, aimed at investigating the saturation behavior of these modes and their adverse impact on particle and energy confinement. A topic of interest is pressure-driven interchange modes, which can be excited when the plasma beta surpasses the Mercier stability criterion. As indicated by prior research in nonlinear MHD simulations for NSTX [Jardin 2022], these excited pressure-driven MHD modes can induce significant thermal transport from the core to the edge, consequently limiting core temperature. Nevertheless, they will not lead to major disruptions like neoclassical tearing modes (NTMs).

In this work, we simulate MTF interchange modes with the M3D-C1 code. We start with linear simulations to determine the threshold for mode excitation and to identify the most unstable modes. We use highly compressed MTF equilibria (C=8) with low shaft current generated using CORSICA as the initial conditions in the M3D-C1 simulations. Fig. 5a shows the equilibrium profile, including the safety factor (q) and plasma pressure. This equilibrium falls within the stable corridor for both the ideal and resistive n=1 modes. For the linear simulation, both the plasma pressure and toroidal mode number (n) are scanned during the search for unstable modes while the q profile is fixed.

The mode growth rates from the simulation are summarized in Fig. 5b. Notably, as core plasma β_0 increases, the mode growth rates rise significantly, indicating a predominantly pressure-driven nature. As β_0 is incremented, high-n modes become unstable while the n = 1 mode remains stable. Figure 6 shows the electromagnetic mode structure and plasma pressure perturbation for n = 6. It reveals the dominant presence of a (9,6) mode, with perturbations in both the electric potential (φ) and plasma pressure localized near $q = q_{min}$, which is not positioned very close to the plasma boundary. This mode structure suggests that the ideal MHD modes are primarily internal modes with substantial pressure perturbations and their excitation is expected to lead to pressure flattening near $q = q_{min}$.

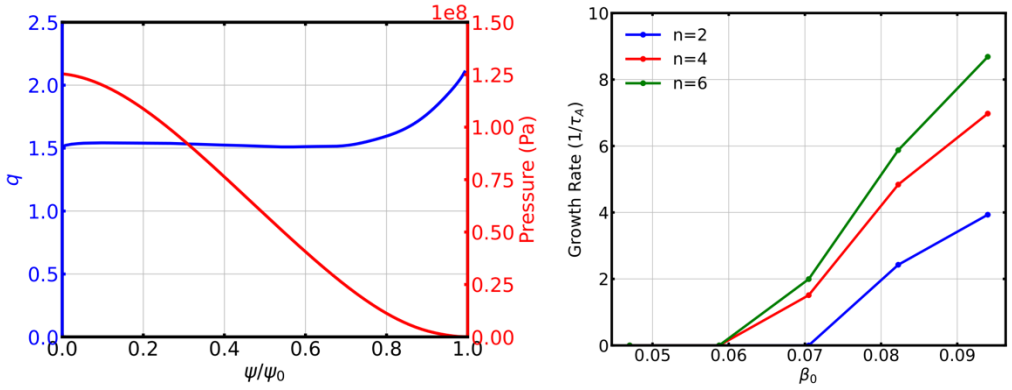

FIG. 5. (a) pressure and q profile of MTF equilibrium used for linear simulation. (b) Linear growth rate of MHD instabilities for different average β and toroidal mode numbers.

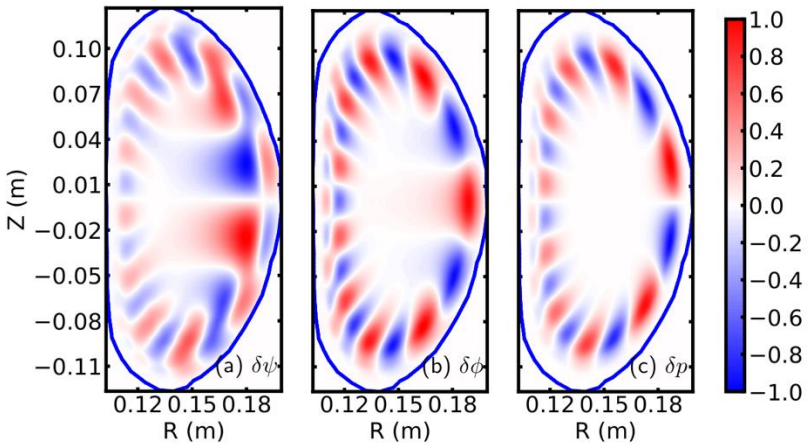

FIG. 6. Mode structure of n = 6 interchange mode from linear M3D-C1 simulation

Based on the linear simulation results, we proceeded to conduct nonlinear simulations, which account for the combined effects of multiple toroidal modes, to study the transport of thermal energy. During the initialization of the nonlinear simulations, we encountered numerical instabilities near the boundaries of the simulation domain that were identified as originating from the low-resolution boundary of CORSICA equilibrium and singularities in the toroidal plasma current distribution. In terms of that, we utilized the CHEASE equilibrium solver to reprocess these equilibria with a high-resolution boundary that aligned with the mesh employed in M3D-C1, effectively mitigating the instabilities.

Figure 7 summarizes the nonlinear simulation for the equilibria with core β_0 = 0.2, including the time evolution of MHD mode magnetic energy for different toroidal mode numbers, alongside the 1D temperature profile at different times. The simulation findings reveal a two-stage behavior in the mode excitation and pressure flattening. In the first stage, n = 3 and n = 4 modes undergo linear excitation followed by nonlinear saturation, causing breaking of magnetic flux surfaces in the outer region (as shown in Fig. 8). However, the temperature profile experiences minimal changes during this stage. In the second stage after 33 μs, all toroidal modes are excited simultaneously resulting in stochastization of magnetic fields throughout the domain. This triggers rapid thermal transport in both the core and edge regions, leading to a substantial alteration of the temperature profile.

The M3D-C1 simulation provides insights into the intricate nonlinear dynamics of interchange modes, highlighting phenomena such as mode-mode coupling and the resultant deconfinement of thermal energy. Importantly, the extent of this effect is closely tied to the occurrence of the second stage, which depends on the excitation of high-n modes. The emergence of rapid magnetic field stochastization in the second stage depends on the saturation level of low-n interchange modes after their linear growth. This result underscores the complex connection between mode excitation and thermal transport and motivates further studies involving nonlinear MHD simulations.

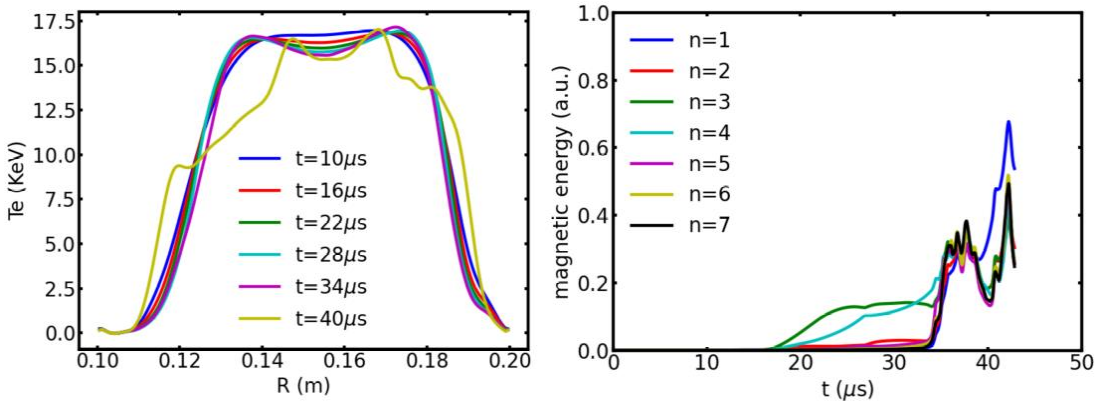

FIG. 7. Time evolution of temperature profile (a) and mode magnetic energy (b) from M3D-C1 nonlinear simulation

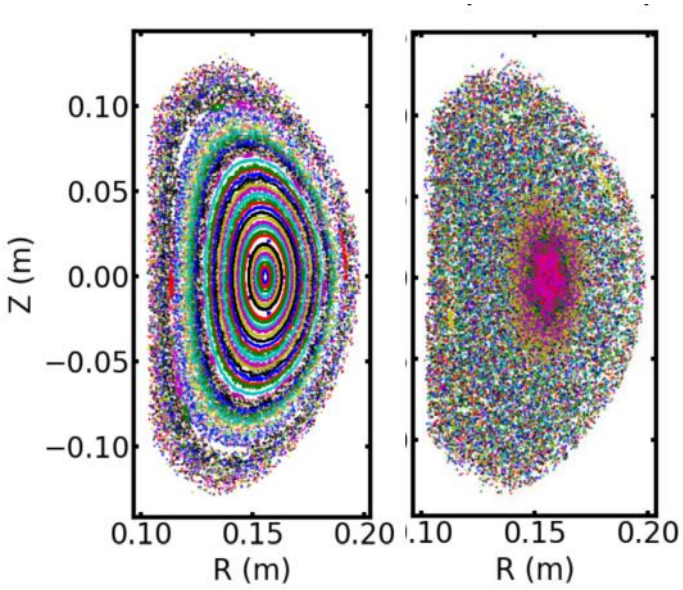

FIG. 8. Poincare plot of magnetic fields at t = 25 μs and t = 40 μs. At 25 μs, linear growth of n=3 and n=4 has caused disruption of the outer flux surfaces. At 40 μs, the entire domain has become stochastic.

C. Error Field Penetration – written by Dylan Brennan

When the axisymmetric plasma is stable to spontaneously growing modes, like those discussed above, externally applied non-axisymmetric magnetic field, or error fields, can still drive instabilities and loss of confinement. In MTF, asymmetries in the confinement device and plasma-liner interface produce error fields. As the plasma is compressed, asymmetries and ripples on the interface become proportionately larger and increasingly affect the plasma. Error

field penetration (EFP) [Finn 2015] is the response of such a plasma to error fields. If the error field is much weaker than the plasma field (typically around a factor of 10^4), then it will be shielded from entering the plasma volume by toroidal rotation. However, as the error field becomes stronger, it penetrates the flux surfaces. This EFP causes damping and eventual locking of the plasma rotation, development of magnetic islands, and stochastization of flux surfaces, all leading to a degradation of the energy confinement [Fitzpatrick 1991, Fitzpatrick 1993a, Fitzpatrick 1993b, Fitzpatrick 1998, Gimblett 1986, Jensen 1993, Nave 1990].

Driven instabilities have been modeled in NIMROD simulations as resonant magnetic perturbations at the boundary (to study the EFP), in the equilibria from our recently published work. Furthermore, a linear layer model for EFP limits [Cole 2006] has been implemented in our analysis framework and was used to calculate the EFP limits in the operational space. This work is now in preparation for publication and will extend the recent results to study the soft beta limits and EFP limits in these cases with idealized geometry. The NIMROD results differ from the results of the analytic model though they share some of the basic characteristics. We do not expect perfect agreement because the analytic model includes only a rudimentary geometric model of the distance between the rational surface and the wall, and no effect from stability. These NIMROD simulations include the effects of linear stability drive and detailed geometry. The plasma models also differ significantly.

In the simulations, the plasma rotation is matched to realistic rates at the core and profiles are based on angular momentum conservation during compression. An error field that is dominantly m/n=2/1 is imposed at the boundary and ramped up over time, starting from a very low level during which early plasma response shields the error field from penetrating. Estimating the island size based on the radial perturbed magnetic field at the resonant surface, we initially get a small island saturating around the linear layer width, as shown in Fig. 9b. As the field continues to increase, eventually the error field penetrates the plasma and a large magnetic island appears, causing stochastic magnetic fields and thermal deconfinement in the simulation. Two Poincare plots are shown of a simulated plasma before and after penetration, respectively. After penetration, the large driven islands are evident along with the stochastic field. The focus of this study is on the magnitude of the applied magnetic field at the boundary when this occurs, under variations of the geometry and plasma parameters during compression.

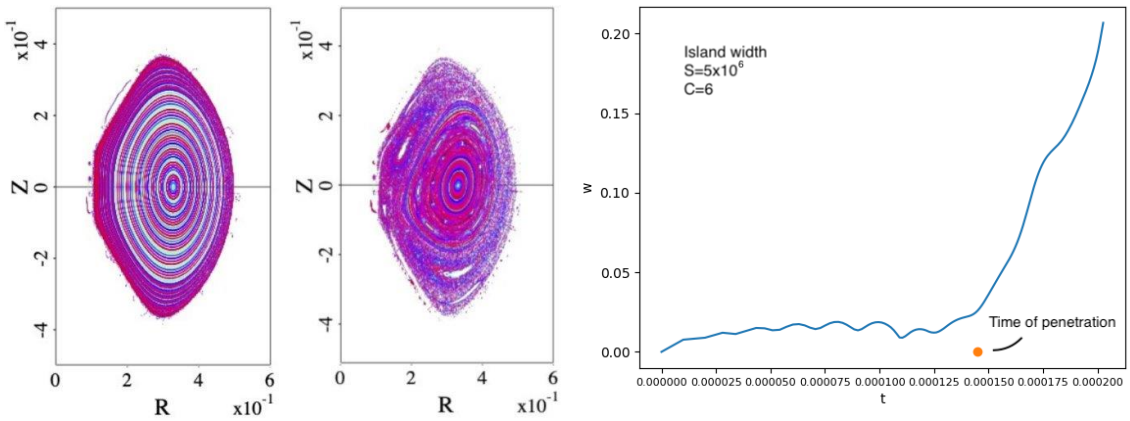

Fig. 9. (Left) Flux surfaces before and after error field penetration (Right) Island width based on radial perturbed magnetic field at the resonant surface.

In Fig. 10 is shown an alternate view of a simulation, where contours of Bz along the outboard midplane are shown as a function of time. The ramping of the boundary condition is evident, as is the initially shielded response at the surface and the penetration.

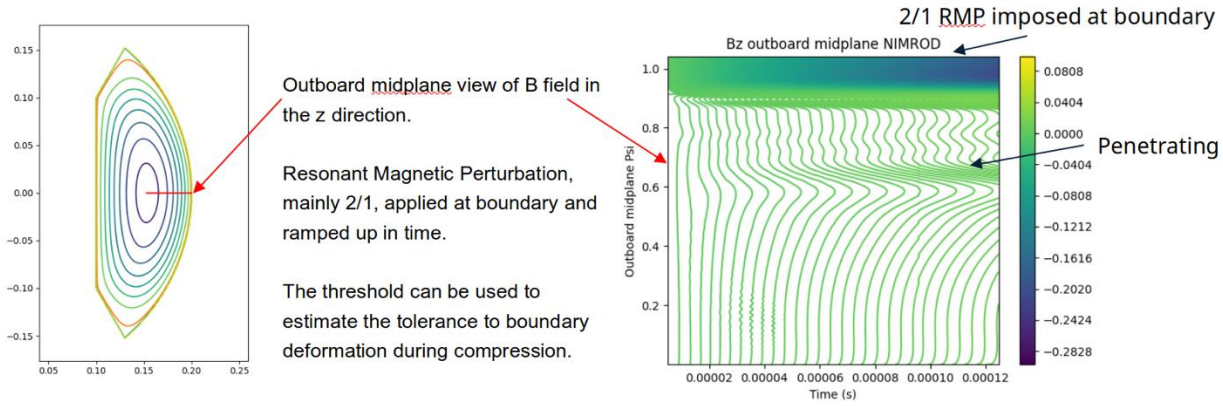

Fig. 10. Contours of Bz along the outboard midplane versus time. When the contours depart from vertical, the axial field on that is ramping at a rate disproportional to the applied fields.

Over the one year of support for this Project, the effect of plasma rotation on the resistive MHD stability of the plasma was investigated with the NIMROD code, and further development of the calculations with RDCON were completed. Penetration thresholds from a series of NIMROD simulations at different S are shown in Fig. 11, plotted as a function of compression ratio C. Cases with higher Lundquist number S have greater thresholds because penetration thresholds tend to increase as the resistive island layer widths increase. Cases at higher compression have greater thresholds because rotation increases and stabilizes the plasma. It was determined that rotation (or toroidal flow) rates of 10^4 rad/s measured in General Fusion's PI3 device effectively stabilize the plasma during compression.

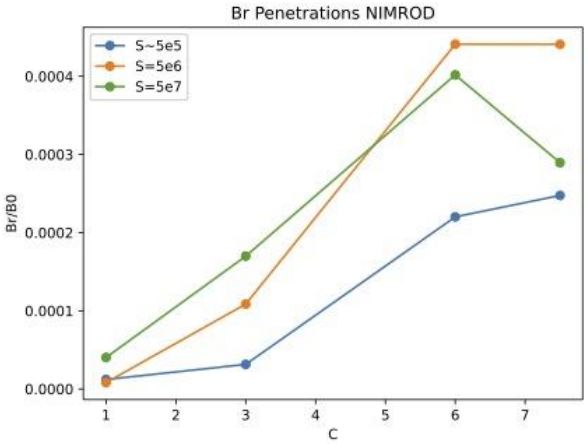

Fig 11. Penetrations thresholds from NIMROD simulations with different Lundquist number, *S*. The threshold tends to increase with compression ratio *C*.

4. POTENTIAL APPLICATIONS, TECHNOLOGY TRANSFER

The application of M3D-C1 and NIMROD to novel devices benefits the entire fusion community. The development and application of these tools to compressing geometries will allow for determination of stable compression trajectories, both for the scheme under development at General Fusion, and for other projects that endeavor to compress magnetized plasmas to fusion conditions. Furthermore, through the study of plasma stability in these configurations, and the verification of RDCON, NIMROD, and M3D-C1 results, a broader range of experience was attained by the research scientists involved with the Project. Most, if not all, of the governing physics and computational techniques are directly applicable to research being conducted on tokamaks such as DIII-D, NSTX-U and ITER. The experience obtained with these simulation tools in a different context (namely General Fusion's compression experiments) will benefit related efforts on these and other tokamak experiments.

The concept of using compression for the heating of closed-flux magnetized plasmas dates back decades. Compression is attractive for heating because of the high power that can be delivered and because compression can be achieved through a liquid metal blanket, as in the General Fusion concept. The heating of tokamak plasmas via magnetic compression has also been studied experimentally on systems such as the Adiabatic Toroidal Compressor [Bol 1972, Bol 1974a, Bol 1974b]. Results from those experiments indicated the onset of MHD modes are a consequence of compression. Many novel fusion concepts, including those supported by ARPA-E, are in various parts of the MTF regime and propose to use similar compact toroid plasma targets. This Project delivered an enhanced modeling toolset for understanding the MHD stability of these magnetized plasma targets during compression, to improve the potential for heating while avoiding MHD instabilities.

5. BENEFITS TO THE FUNDING DOE OFFICE'S MISSION

Understanding the stability of magnetized plasma has been a significant challenge of physics for many decades and is still a subject of intense research at national laboratories. Princeton

Plasma Physics Laboratory (PPPL), in particular, is at the forefront of this research. This Project contributed to broader understanding of fusion plasma stability, particularly in MTF devices, and contributed to the development of numerical codes able to model that efficiently. As MTF can be classified as a special case of a spherical tokamak, the study here offers valuable insights for future research on NSTX-U and spherical tokamak-based fusion power plants. It also strengthens the collaboration between GF and PPPL, benefiting both parties by cross-fertilization of ideas and codes benchmarking.

REFERENCES

[Bol 1972] K. Bol et al. Adiabatic compression of the tokamak discharge. Phys. Rev. Lett., 29:1495–1498, 1972.

[Bol 1974a] K. Bol et al. Experiments on the Adiabatic Toroidal Compressor. PPPL Technical Report, 1974. doi:10.2172/4203067.

[Bol 1974b] K. Bol et al. Experiments on the Adiabatic Toroidal Compressor. Fifth IAEA Conference Proceedings, Tokyo, Plasma Phys. and Controlled Nucl. Fusion, 1:83, 1974.

[Brennan 2014] D. P. Brennan and J. M. Finn. Control of linear modes in cylindrical resistive MHD with a resistive wall, plasma rotation, and complex gain. Physics of Plasmas, 21(10):102507, 2014.

[Chandra 2005] D Chandra, A Sen, P Kaw, M.P Bora, and S Kruger. Effect of sheared flows on classical and neoclassical tearing modes. Nuclear Fusion, 45(6):524–530, May 2005.

[Chen 1990] X. L. Chen and P. J. Morrison. Resistive tearing instability with equilibrium shear flow. Physics of Fluids B: Plasma Physics, 2(3):495–507, 1990.

[Chu 1999] M.S Chu, L Chen, L.-J Zheng, C Ren, and A Bondeson. Effect of rotation on ideal and resistive MHD modes. Nuclear Fusion, 39(11Y):2107–2111, Nov 1999.

[Cole 2006] A. J. Cole and R. Fitzpatrick, Phys. Plasmas 13, 032503 (2006).

[Crotinger 1997] J.A. Crotinger et al. CORSICA: A comprehensive simulation of toroidal magnetic-fusion devices. Final report to the LDRD Program. LLNL Report, UCRL-ID-126284, 1997.

[Finn 2015] John M. Finn, Andrew J. Cole, Dylan P. Brennan; Error field penetration and locking to the backward propagating wave. *Phys. Plasmas* 1 December 2015; 22 (12): 120701. https://doi.org/10.1063/1.4939211

[Fitzpatrick 1991] R. Fitzpatrick and T. C. Hender, Phys. Fluids B 3, 644 (1991).

[Fitzpatrick 1993a] R. Fitzpatrick, Nucl. Fusion 33, 1049 (1993).

[Fitzpatrick 1993b] R. Fitzpatrick, R. J. Hastie, T. J. Martin, and C. M. Roach, Nucl. Fusion 33, 1533 (1993).[7] A. H. Boozer, Phys. Rev. Lett. 86, 5059 (2001).

[Fitzpatrick 1998] R. Fitzpatrick, Phys. Plasmas 5, 3325 (1998).

[Froese 2018] A. Froese, D. Brennan, M. Reynolds, and M. Laberge. MHD Stability of a Magnetized Target During Non-Self-Similar Compression [Poster]. APS Div. Plasma Physics 2018. https://generalfusion.com/2018/11/mhd-stability-magnetized-target-non-self-similar-compression.

[Gimblett 1986] C. G. Gimblett and R. S. Peckover, Proc. Royal Soc. of London Series A 368, 75 (1986).

[Glasser 2016a] A.H. Glasser. The direct criterion of Newcomb for the ideal MHD stability of an axisymmetric toroidal plasma. Physics of Plasmas, 23:072505, 2016.

[Glasser 2016b] A.H. Glasser, Z.R. Wang, and J.-K. Park. Computation of resistive instabilities by matched asymp- totic expansions. Physics of Plasmas, 23:112506, 2016.

[Hao 2014] G. Z. Hao et al. Finite toroidal flow generated by unstable tearing mode in a toroidal plasma. Physics of Plasmas, 21(12):122503, 2014.

[Jardin 2004] S.C. Jardin. A triangular finite element with first-derivative continuity applied to fusion MHD applications. J. Comp. Phys., 200(133):133, 2004.

[Jardin 2022] S.C. Jardin, N.M. Ferraro, W. Guttenfelder, S.M. Kaye, and S. Munaretto. Ideal MHD Limited Electron Temperature in Spherical Tokamaks. Phys. Rev. Lett. **128**(24), 245001 (2022).

[Jensen 1993] T. H. Jensen, A. W. Leonard, A. W. Hyatt; A simple model for driven islands in tokamaks. *Phys. Fluids B* 1 April 1993; 5 (4): 1239–1247. https://doi.org/10.1063/1.860913

[Laberge 2008] M. Laberge. An Acoustically Driven Magnetized Target Fusion Reactor. Journal of Fusion Energy, 27:65–68, 2008.

[Li 2017] L. Li et al. Effects of magnetic islands on resonant field penetration and toroidal torques at slow plasma flow. Nuclear Fusion, 57(12):126027, 2017.

[Liu 2008] Y.Q. Liu, M.S. Chu, I.T. Chapman, and T.C. Hender. Toroidal self-consistent modeling of drift kinetic effects on the resistive wall mode. Physics of Plasmas, 15:112503, 2008.

[Nave 1990] M. F. Nave and J. A. Wesson, Nucl. Fusion 7, 2575 (1990).

[Sovinec 2004] C.R. Sovinec et al. Nonlinear Magnetohydrodynamics with High-order Finite Elements. J. Comp. Phys., 195:355, 2004.

[Tóth 1996] G Tóth. A general code for modeling MHD flows on parallel computers: Versatile Advection Code. Astrophysics Letters and Communications, 34:245, 1996.

[Wang 2018] Z.R. Wang, J.-K. Park, J.E. Menard, Y.Q. Liu, S.M. Kaye, and S. Gerhardt. Drift kinetic effects on plasma response in high beta spherical tokamak experiments. Nuclear Fusion, 58:016015, 2018.

[Weller 1998] H. G. Weller et al. A tensorial approach to computational continuum mechanics using object-oriented techniques. Computers in Physics, 12(6):620–631, 1998. https://openfoam.org.